

Optimization of Reaction Conditions for Green Synthesis of Silver Nanoparticles Using *Coffea Arabica* Leaf Extract

ABSTRACT

Present study describes a rapid and eco-friendly synthesis of silver nanoparticles (AgNPs) using *Coffea Arabica* leaf extract in single process via green Chemistry. We have successfully synthesized AgNPs using *Coffea Arabica* leaf as a reductant and a capping or stabilizing agent through green chemistry. In the typical synthesis of AgNPs, *Coffea Arabica* leaf extract was added into aqueous solution of AgNO_3 in a conical flask at 80°C temperature. Different reaction concentrations of *Coffea Arabica* extract and AgNO_3 solution were subjected. AgNPs were synthesized by using aqueous silver nitrate solution as a precursor with aqueous solution of *Coffea Arabica* leaf extract as the reductant and stabilizing agents. The AgNPs were characterized using Fourier transform infrared spectroscopy (FTIR), X-Ray Diffraction (XRD), Atomic Absorption Spectroscopy (AAS) and UV-Vis spectroscopy. The optimum conditions for this process were a temperature of 80°C , pH 9, and reactant ratio 1:4. XRD results reveal that, the green synthesis yields stable, face centered cubic structure AgNPs with a sizes range of 39.664-24.708 nm. Preparation of AgNPs using plant extracts are eco-friendly, biocompatible and cost effective. The synthesis method applied in this study involved the application of the green chemistry principles which emphasizes on the use of nontoxic solvents and reagents to protect the environment. AgNPs have a vital role in different nanotechnology-based processes because of their unique characteristics and can be exploited on a large scale for medical application.

Keywords: Coffea Arabica; Green synthesis; Aqueous Extract; Nanoparticles

1. INTRODUCTION

“Green chemistry is a significant field of research as it offers simple, cost-effective, easy, biocompatible and eco-friendly methods for the synthesis of nanomaterials in the field of nanotechnology” [1].

35 "Nanotechnology" is the newest and one of the most promising and active areas of modern research. The
36 technology deals with the design, synthesis, and manipulation of particles size ranging from 1–100 nm
37 [1]. "Within this size range, the chemical, physical, and biological properties change in the fundamental
38 way of both individual atoms and their corresponding bulk material" [2]. This very small size increases the
39 surface area-to-volume ratios of particles. The nanoparticles synthesized using plant extract have gained
40 huge consideration in recent years due to their remarkable properties and wide range of applications in
41 catalysis [3], plasmonic [4], optoelectronics [5], biological sensor [6], water treatment, pharmaceutical
42 applications [7], and agriculture and crop protection [8]. "Stunning growth in this emerging technology has
43 opened novel fundamental and applied frontiers, including the synthesis of nanomaterial and utilization of
44 their physicochemical and optoelectronic properties" [9]. "The application of nanotechnology has
45 increased in large number of areas such as optics, mechanics, chemical industries, space industries,
46 electronics, energy science, single electron transistors, light emitters, nonlinear optical devices, photo-
47 electrochemical, catalysis, biomedical, cosmetics, drug delivery, and food and feed" [10-14].

48 "Due to their exceptional biological and physicochemical properties, metal nanoparticles (NPs) have
49 devoted particular attention to their use in emerging constituents for various applications" [15]. "Among
50 several metal nanoparticles, silver nanoparticles (AgNPs) are one of the most dynamic and interesting
51 nanomaterials that have gained significant attention in the arena of nanotechnology" [16]. "AgNPs and
52 their nanocomposites have created marvelous potential and noteworthy applications in diverse fields of
53 nanotechnology, particularly in biomedical therapeutic researches, MRI contrast agents, drug delivery,
54 and biomedical devices for the detection of numerous alarming diseases or complications" [17].
55 "Moreover, AgNPs have a wide range of use because of their unique characteristics such as optical,
56 electrical and magnetic properties, which can be incorporated into antibacterial, antiviral, and antifungal
57 applications, composite fibers, biosensor materials, cosmetic products, food industry uses, and electronic
58 components" [18, 19]. "AgNPs are also reported as medical and pharmaceutical agents that have directly
59 encountered by a human system in such products as shampoos, detergents, soaps, toothpaste, and
60 cosmetics" [20]. The biomedical use of AgNPs includes their application as antibacterial [21], antifungal
61 [22], anti-inflammatory [23,24], antiviral [25], and anti-diabetic agents [26].

62 "In the intensive search for a good biological agent for synthesizing metal nanoparticles, several biological
63 entities from microbes to plants and animal products have been given much attention" [27-29]. "Among
64 the different bio-tools used to produce nanoparticles, plant extracts are given high priority" [30-32]. "Green
65 synthesis routes using various plants have produced active materials that have greater potential against
66 gram-positive and gram-negative microorganisms and different cancer cell lines and exhibit higher
67 antioxidant effects than those produced by chemical and thermal physical methods" [33-35].

68 In recent studies, green synthesis of AgNPs using extracts of *Garcinia mangostana* [36], *Lepidium draba*
69 [37], *Crocus Hausknechtii* Bois [38], *Mimusops elengi* [39], *Boerhaaviadiffusa* [40], *Meliadubia* leaf [41],
70 *Pistacia atlantica* [42], *Momordica cymbalaria* [43], *Mentha aquatica* [44], *Parquetina nigrescens* and

71 *Synedrella nodiflora* [45], *Terminalia chebula* [46], *Costus afer* [47], *Ormocarpum cochinchinense* [48],
72 *Callistemon citrinus* [49], and *Tectona grandis* [50] have been reported. In addition to the previous
73 reports, a wider range of applications of bio-inspired synthesized AgNPs has been reported.

74 The current study focuses on the synthesis and characterization of AgNPs from *Coffea Arabica* leaf
75 extract. Green synthesis was a method utilized for the preparation of AgNPs and was characterized via:
76 UV-visible spectroscopy, Atomic Absorption Spectroscopy (AAS), X-ray diffraction (XRD), Fourier
77 transform infrared spectroscopy (FTIR), and Scanning Electron Microscope (SEM) analysis. The results
78 of this study will have a significant role in the scientific knowledge of plant mediated synthesis of
79 nanoparticles. The synthesis method applied was green chemistry which emphasizes on the use of
80 nontoxic solvents and reagents to protect the environment. The novelty of this study is that it is the first
81 report of the synthesis of AgNPs using *Coffea Arabica*. As far as our knowledge is concerned, there is no
82 any report regarding the green synthesis of AgNPs using *Coffea Arabica* leaf extract.

83 2. MATERIALS AND METHODS

84 2.1. Preparation of the Leaf Extracts

85 For the preparation of the aqueous extract, fresh green leaves of *Coffea Arabica* was used. Some
86 amount of *Coffea Arabica* leaves were weighed, washed with tap water followed by distilled water to
87 remove all the dirt. Then the clean leaf was shade dried, grounded using mortar and pestle, and boiled in
88 250 ml of distilled water at 80°C for 3 minutes. Finally, the solution was cooled and filtered with What-man
89 No.1 filter paper and thus, the aqueous extract was kept at 4°C for AgNPs preparation [51].

90 2.2. Preparation of AgNO₃ solutions

91 AgNO₃ was carefully weighed using analytical balance and then transferred into 1000 ml volumetric flask
92 that contained 400 ml of distilled water. The solid material was completely dissolved and distilled water
93 was added to fill up to the mark. A 0.004 M solution of AgNO₃ was prepared in an amber bottle and stored
94 in a cool and dry place [52].

95 2.3. Green Synthesis of AgNPs

96 In the typical synthesis of AgNPs, aqueous *Coffea Arabica* leaf extract (20 g/250 ml) was added into the
97 aqueous solution of 4 mM AgNO₃ in a conical flask at 80 °C. Different reaction concentrations of *Coffea*
98 *Arabica* extract and AgNO₃ solutions were subjected. Ag ion was reduced into Ag metal. The prepared
99 AgNPs were characterized using XRD, FTIR, SEM, AAS and UV-Vis spectroscopy [53].

100 2.4. Spectrophotometric Analysis of the Samples

101 UV-Vis spectroscopy refers to the absorption/emission in the range of UV-Vis spectral region. Usually,
102 350–700 nm light is used for the characterization of 2–100 nm sized metal nanoparticles [54]. UV-vis
103 spectroscopy is an instrument that can be used to evaluate the formation and stability of AgNPs in
104 aqueous solution [55]. Spectrophotometric absorption measurements in the wavelength ranging from 380
105 up to 500 nm commonly use to characterize silver nanoparticles [56]. In this work a double beam UV-Vis

106 instrument with a scan rate of 4800 nm/min at a wavelength range of 350-700 nm was used and the
107 spectroscopic analysis was done using Cary 60 version 2.

108 **2.5. FTIR and XRD Analysis of AgNPs**

109 FTIR studies were carried out using a shimadzu spectrophotometer (model 100, Japan). The samples
110 were synthesized using KBr pellet method and *Coffea Arabica* leaf extract as well as the synthesized Ag
111 nanoparticles were analyzed for the presence of bio-functional moieties under optimized conditions. FTIR
112 spectra of AgNPs were recorded at a resolution of 2 cm^{-1} in transmission mode between 3500 and 650
113 cm^{-1} . XRD pattern of synthesized nanoparticles was also done by using DX-2700 X-Ray Diffractometer.
114 The X-ray source was obtained in Cu- K_{α} radiation with 0.154 nm wavelength. The XRD system was run at
115 30 mA current and 40 KV voltage and the nanomaterials were scanned in the range of 3 - 80°.

116 **2.6. AAS Analysis of AgNPs**

117 The conversion of Ag ion to Ag metal can be inferred with this measurement. The aliquant sample was
118 withdrawn and shaken at regular interval during the reaction. The supernatant solution contains the
119 unreacted AgNO_3 for the reason that Ag ions are so much smaller than Ag metal and the pellets contain
120 AgNPs. The supernatant solution was examined using AAS to identify the concentration of Ag ions. The
121 reduction rate of the concentration of Ag ion was exhibited the conversion of Ag ion into Ag metal.

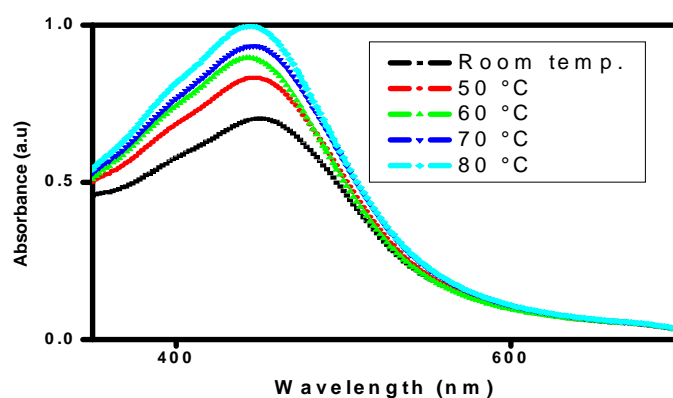
122 **3. RESULTS AND DISCUSSION**

123 **3.1. UV-Visible Spectroscopy Characterization**

124 **3.1.1. Effect of Temperature on the synthesized AgNPs**

125 Temperature is a physical factor that plays a great role in controlling the nucleation reaction of
126 nanoparticles fabrication. The absorbance of silver nanoparticle was recorded at a temperature 25°,
127 50°, 60°, 70° and 80°C. On the basis of UV-Vis studies better synthesis was demonstrated at 80°C.

128 UV-visible absorption spectra have been used to prove its significance and sensitivity towards silver
129 colloids formation since AgNPs display an intense absorption peak as a result of the Surface Plasmon. As
130 shown in figure 1 below, a wide peak was observed at 450 nm and 25°C for the reaction mixture.
131 Broadening of band attributed to the agglomeration and increase in size of the particles [57]. Increase in
132 absorbance increases the temperature from 25 to 80° and the bands become narrow. Moreover;
133 nanoparticles synthesized at higher temperature increase the rate of formation of AgNPs, retarding the
134 secondary reduction process. Others study by [58] also reported similar result and attributed the trend to
135 the increase in solubility of the phenolic at higher temperature. Increasing the absorbance of the reaction
136 mixture increases the incubation temperature markedly showing higher productivity of AgNPs, at elevated
137 temperature. The sharpness of absorbance peak depends on the size of the nanoparticles. The
138 nanoparticle size become smaller when the temperature is higher, resulting in sharpness of the Plasmon
139 resonance band of silver nanoparticles [59].



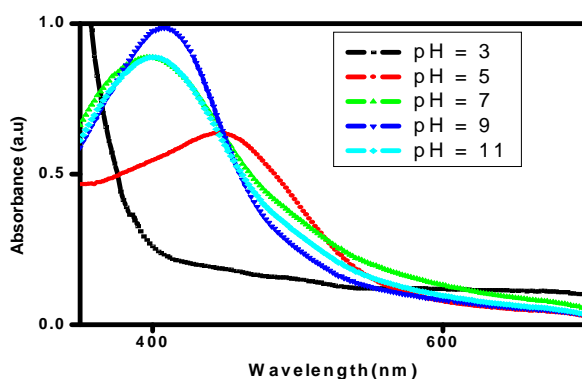
140

141 **Fig. 1. UV-Vis absorption spectra of the synthesized AgNPs at different temperatures**

142 **3.1.2. Effect of pH on the synthesized AgNPs**

143 Preparation of AgNPs using *Coffea Arabica* leaf was conducted over a pH range of 3–11. Fig.2 shows
 144 that the UV-Vis spectra of Ag nanoparticles extracted from *Coffea Arabica* leaf and the effect of the
 145 variation in pH.

146 The UV-Vis absorption peak was very wide at pH five as indicated in Fig.2. This wide result may be
 147 because of increase in AgNPs size. The presence of larger nanoparticles and platelets at lower pH can
 148 be attributed to the uncontrolled nucleation as well as aggregation because of the improved interaction of
 149 negatively charged ions. Another study was also reported, at low pH, the aggregation of AgNPs to form
 150 larger nanoparticles was believed to be favored over the nucleation to form new nanoparticles [60]. An
 151 efficient AgNPs were prepared at pH 9 and the size remained smaller but agglomeration AgNPs was
 152 noticed at pH 11, therefore pH 9 was the optimal value for efficient AgNPs synthesis. Our result agreed
 153 with what was reported by [61]. At higher pH, however, the large number of functional groups available
 154 for silver binding facilitated a higher number of Ag to bind and subsequently form a large number of
 155 nanoparticles with smaller diameters. In addition at higher pH the shape of the nanoparticles formed were
 156 more of spherical in nature rather than ellipsoidal. There was no formation of silver nanoparticles at pH <
 157 5, this might be due to the instability of the nanoparticles at lower/acidic pH [62]. Acidic conditions avoid
 158 the formation of AgNPs whereas, basic conditions enhance the formation of AgNPs. This result confirmed
 159 the very important role played by pH in controlling the shape and size of the AgNPs synthesis.

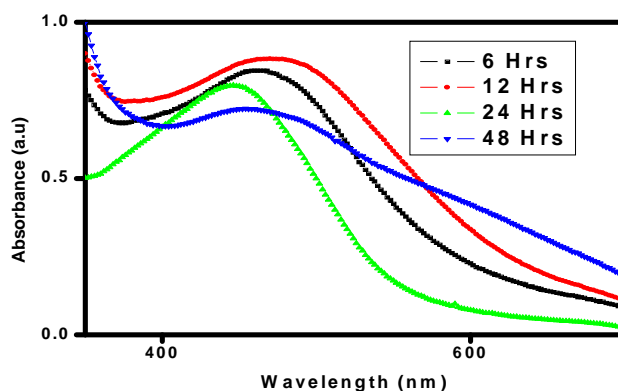


160
161

Fig. 2. UV-Vis absorption spectra of the synthesized AgNPs at different pH values

162 **3.1.3. Effect of reaction time on the synthesized AgNPs**

163 The reaction between reducing agent and Ag ion was run for 6, 12, 24 and 48h at room temperature. The
 164 color change of the solution from yellow to brownish-yellow and then to deep brown indicates that the
 165 synthesis of AgNPs when 4mM AgNO₃ was added to *Coffea Arabica* leaf extract at different time interval.
 166 Figure 3 shows the UV-Vis absorption spectra of the colloidal solution. It should be noted that the
 167 intensity of the color of the reaction mixture was directly proportional to the incubation time due to
 168 excitement in the surface Plasmon resonance phenomenon. The maximum absorbance was observed at
 169 12h time interaction. When the absorbance was increased, the interaction time of Ag ions with *Coffea*
 170 *Arabica* leaf extract was also increased. UV-Vis spectra in figure 3 shows that the best synthesis was
 171 obtained at 12h of incubation. The obtained results demonstrated that the higher the absorbance the
 172 more AgNPs formed as the reaction time increases to 12h and similar results were also reported by [63].
 173 An optimum period is required due to the unsteadiness of the AgNPs synthesis, as agglomeration after
 174 optimum time interval resulting in larger sizes of particles. As absorption increases, the incubation time
 175 increases from 6 to 12h. Agglomeration of AgNPs was occurred after the optimum time due to the
 176 instability of the nanoparticles, therefore, maximum time was required to form larger particle size [64].



177
178

Fig. 3. UV-Vis absorption spectra of the synthesized AgNPs at different reaction time

3.1.4. Effect of concentration on the synthesized AgNPs

The absorbance peak (454 nm) of *Coffea Arabica* leaf extract was broad and less intense as shown in Fig.4 at 5 g/250 ml leaf extract concentration. However, as the *Coffea Arabica* leaf extract concentration increases gradually from 5 g/250 ml to 20 g/250 ml, the absorbance peak becomes narrower and more intense. There was gradual increase in absorbance as the *Coffea Arabica* leaf extract concentration increases. Based on the UV-Vis studies, the synthesis of AgNPs was better demonstrated at 20 g/250 ml. At lower extract concentrations, a lesser number of nucleation sites were present so more reduction were taken place at single nuclei leading. At higher concentration the polyphenols in the *Coffea Arabica* leaf extract were effectively reduced from Ag-ions to Ag⁰ and provide enough capping agent for the stabilization of the synthesized nanoparticles through steric hindrance. Thus preventing their aggregation, which probably leads to the formation of smaller particles at a higher concentration [65]. These results were agreed with what was reported before [66].

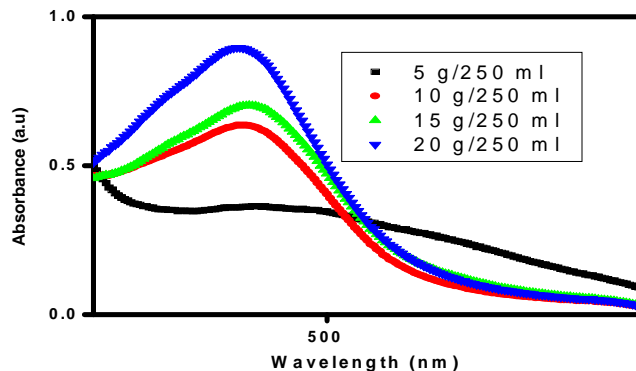
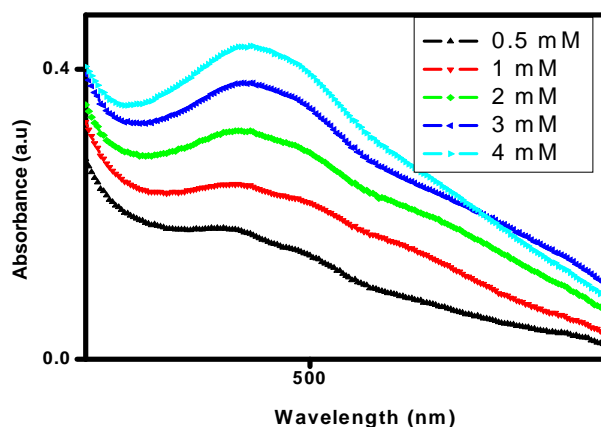


Fig. 4. UV-Vis absorption spectra of the synthesized AgNPs at different concentration

3.1.5. Effect of silver ion concentration on the synthesized AgNPs

Various concentration such as 0.5, 1, 2, 3 and 4mM AgNO₃ were taken for the optimum preparation of nanoparticles. Interestingly 4mM concentration supported rapid formation compared to the other concentrations (Fig. 5). When the concentration of AgNO₃ was increased the number of AgNPs were risen. When AgNO₃ concentration was increased from 0.5 up to 4mM, the yield of AgNPs were also increased. Hence 4mM concentration of AgNO₃ was chosen for further experimentation. The concentration of metal ion has an essential role in the nanoparticles production. Similar effect of varying concentration of silver salt on yield, size and disperse of AgNPs was reported by others [67].

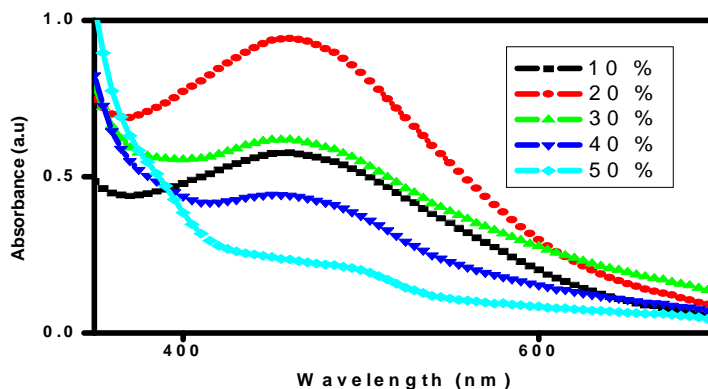


201
202

203 **Fig. 5. UV-Vis absorption spectra of the synthesized AgNPs at different Ag ion concentration**

204 **3.1.6. Effect of Reactants Ratio on the synthesized AgNPs**

205 Different volume (10, 20, 30, 40 and 50 ml) of plant extracts were added to 4mM AgNO₃ aqueous solution
 206 at room temperature. The solutions were characterized using UV-Vis after 12h. Figure 6 shows that the
 207 UV-Vis spectra of AgNPs at different volume of *Coffea Arabica* leaf extract (10-50ml). A maximum
 208 absorbance was observed at 20ml *Coffea Arabica* leaf extract with narrow peak. The absorbance
 209 increases with increasing the volume *Coffea Arabica* leaf extract, and reached maximum at 20ml, then
 210 start to decrease from 30 – 50 ml. UV-Vis spectra (Fig.4) indicated that 20ml *Coffea Arabica* leaf extract
 211 yielded best result. The optimal concentration of the reactant ratio was 1:4. The obtained results support
 212 similar finding reported by [68]. The stability of the colloidal solution was influenced by the absorbing
 213 species present and concentration of reducing agents [69].

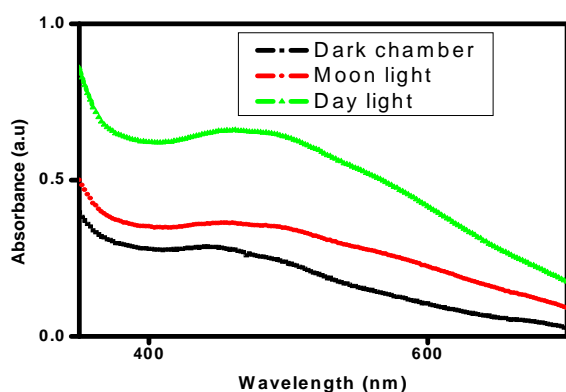


214
215

Fig. 6. UV-Vis absorption spectra of the synthesized AgNPs at different ratio of reactants (v/v %)

216 **3.1.7. Effect of Light on the synthesized AgNPs**

217 Effect of light on the rate of AgNPs synthesis clearly demonstrated better synthesis in sunlight compared
218 with other light sources such as moonlight and dark room. Sunlight was an essential source for the
219 synthesis of the nanoparticles and used as photosensitization of the molecules present in the plant
220 extract. Figure 7 shows that the UV-Vis absorption spectra of synthesized AgNPs at different light
221 sources. When the reaction mixture was kept in dark overnight no color change was observed and the
222 synthesis was delayed, similar findings were reported by others [70]. Current study showed that light is
223 significantly executing for green synthesis of AgNPs from the leaf extract.



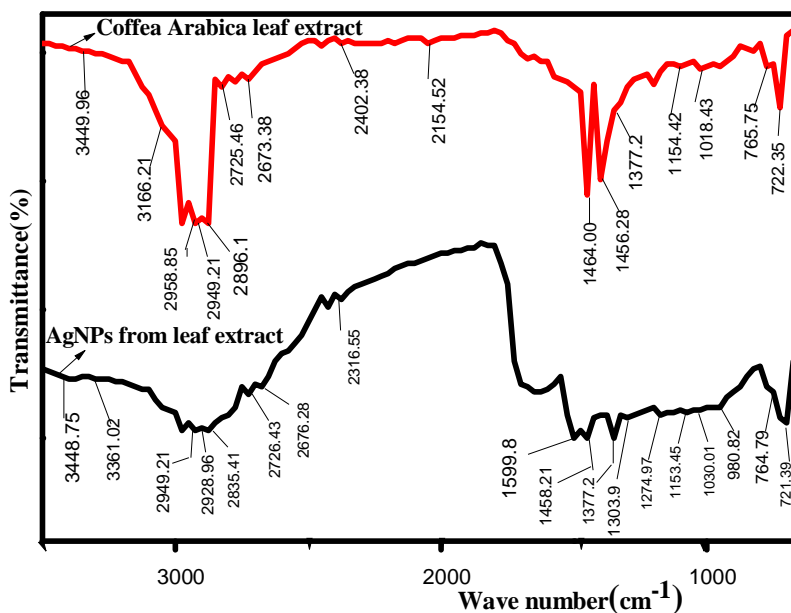
224
225

226 **Fig. 7. UV-Vis absorption spectra of the synthesized AgNPs at different light sources**

227 **3.2. FTIR Analysis**

228 Figure 8 shows the FTIR spectra of *Coffea Arabica* leaf extract and synthesized AgNPs. FTIR
229 measurement of *Coffea Arabica* leaf extract and synthesized AgNPs were carried out to identify the
230 functional groups present and proteins surrounding as stabilizing agent. The sample contains alcoholic,
231 phenolic and carboxylic groups indicating that broadband around 3440 cm^{-1} corresponding to O–H
232 stretching of hydroxyl group. Moreover; primary and secondary amines and amides were signified by N–H
233 stretching. This band can be attributed to the non-dissociative adsorbed water molecules as well as the
234 presence of N-H stretching can prove the presence of band at 1600 cm^{-1} due to the vibration of water
235 molecules. The peak around 1154 cm^{-1} is ascribed to C–N stretching of aromatic and the bands at 900--
236 700 cm^{-1} correspond to primary and secondary amines and amides (--NH_2 wagging). The presence of
237 ketones, aldehydes, quinines and esters can be shown by the peaks around 1600 cm^{-1} assigned to the
238 C=O vibration of carbonyl groups. The band at 2949 cm^{-1} is attributed to C–H stretching of alkanes. The
239 band at $2310, 2154, 1377$ and 1018 cm^{-1} attributed to the strong stretching of C–N aromatic and aliphatic
240 amines. The peak at 1600 cm^{-1} is attributed to C=C vibration of aromatic structure whereas the peak at
241 1274 cm^{-1} is assigned to C–O stretching of phenolic groups. Another broadband centered around 1030
242 cm^{-1} is attributed to the aromatic ethers and polysaccharides (C–O–C) stretch [71]. Carbonyl groups
243 proposed the presence of OH functional groups and proteins show the presence of phenolic compounds

244 in the *Coffea Arabica* leaf extracts. After AgNPs formation, there were some shift of valuable peaks such
 245 as the O–H vibration from 3449.96 cm⁻¹ to 3448.75 cm⁻¹, N–H vibration from 2958.85 cm⁻¹ to 2949.21 cm⁻¹
 246 , 2725.46 cm⁻¹ to 2726.43 cm⁻¹, C–N vibration from 1456.28 cm⁻¹ to 1458.21 cm⁻¹ and 1154.42 cm⁻¹ to
 247 1153.45 cm⁻¹, and disappearance of peaks 2154.52 cm⁻¹ indicating that reduction occurred.



248
 249 **Fig. 8. FTIR spectra of *Coffea Arabica* leaf extract and synthesized AgNPs**

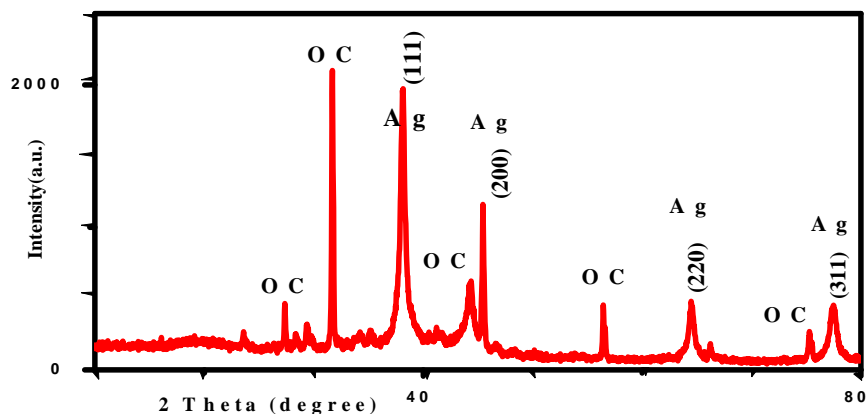
250 3.3. XRD Analysis

251 The crystalline nature of the AgNPs formed was confirmed. XRD spectra of silver the synthesized
 252 nanoparticles are displayed in figure 9. The XRD pattern shows that, the structure of AgNPs is face-
 253 centered cubic [72]. The XRD analysis of synthesized silver nanoparticles had four peaks at 38.115°,
 254 44.229°, 64.443°, 77.4° which corresponds to (1 1 1), (2 0 0), (2 2 0), (3 1 1) diffraction peaks. Sharp
 255 peak of (1 1 1) with high intensity was observed depicting thin film formation on the substrate. This agrees
 256 with previous report [73]. The sharp bands of Bragg's peak showed that the particles were in Nano form
 257 and stabilized by the reducing agents in the *Coffea Arabica* leaf extract. Additionally, the Bragg's peak
 258 shows the representation of silver nanocrystals. The XRD pattern also shows additional peaks due to the
 259 organic compounds present in the *Coffea Arabica* leaf extract and responsible for silver reduction and
 260 stabilization of the resulting nanoparticles [74]. Hence from the XRD pattern, it is clear that AgNPs formed
 261 by the reduction of Ag-ions using *Coffea Arabica* leaf extract were essentially crystalline. The crystallite
 262 size was calculated by using the Debye Scherer's formula [75].

$$d = \frac{K\lambda}{\beta \cos(\theta)} \quad (3.1)$$

263 Where D is the average crystallite domain size perpendicular to the reflecting planes, k is Debye
 264 Scherer's constant (K=0.9), λ is the X-ray wavelength (0.15406 nm), β is udefull width at half maximum

265 (FWHM), and θ is the diffraction angle. The average crystallite size according to Scherer's equation
266 calculated was found to be 29.3 nm.

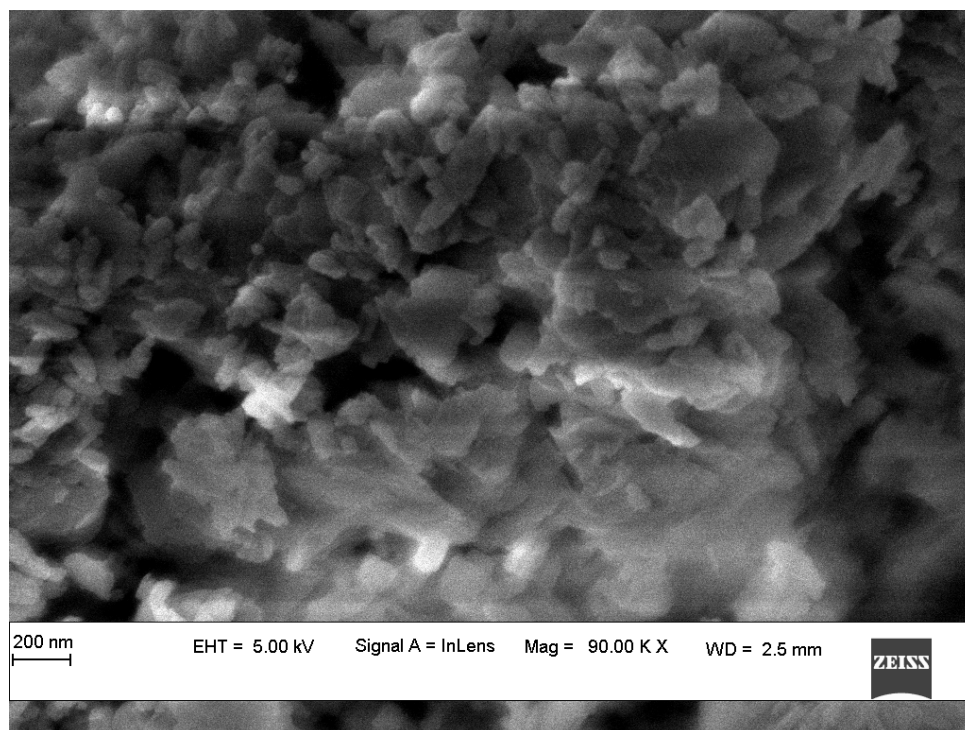


267
268 **Fig. 9. X-ray diffraction pattern of the synthesized AgNPs**

269 3.4. Scanning Electron Microscopy (SEM) Analysis

270 The morphology of the synthesized AgNPs were analyzed using FESEM as shown in figure 10. The
271 FESEM image revealed that AgNPs spherical shapes were well dispersed. Some of the nanoparticles
272 were oval shape due to this it was very difficult to measure the particle size. The biosynthesized AgNPs
273 were dispersed in the solution as reported by Saba et al, 2019 [76].

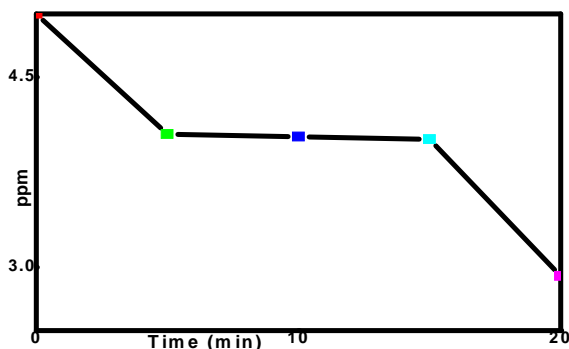
274



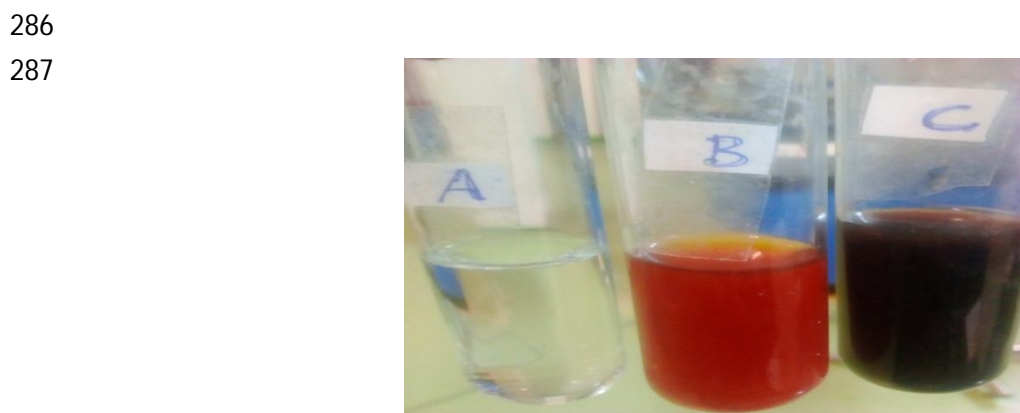
275
276 **Fig. 10. SEM diagram of the synthesized AgNPs**

277 3.5. Atomic Absorption Spectroscopy (AAS)

278 Figure 11 shows the graph of Ag-ion concentration in the reaction mixture conducted by AAS. AAS
279 analysis was done at regular time intervals and the conversion of Ag-ions into silver metal was observed.
280 Initially, a standard solution of 5.0 ppm of AgNO₃ was prepared and analyzed using AAS. Then, Ag-ion
281 concentration in the solution was monitored at regular time intervals after adding Coffea Arabica leaf
282 extract. Result indicated that decreasing in concentration of Ag-ions (5.0, 4.05, 4.03, 4.01 and 2.93 ppm)
283 at 0, 5, 10, 15 and 20 min. respectively exhibiting the conversion of Ag-ion to Ag metal.



284
285 Fig. 11. Graph of Ag-ion concentration in the reaction mixture



288
289 Fig. 12. Color change of the leaf extract: A) 4mM AgNO₃ solution (colorless) B) aqueous extract of
290 Coffea Arabica leaves (yellowish brown) C) synthesized AgNO₃ (deep brown)

291 4. CONCLUSIONS

292 In conclusion, present study describes a rapid and eco-friendly synthesis of AgNPs using Coffea Arabica
293 leaf extract in single process via green Chemistry. We have successfully synthesized AgNPs using
294 Coffea Arabica leaf as a reductant and a capping or stabilizing agent through green chemistry. The
295 optimum conditions for this process were a temperature of 80 °C, pH 9, and reactant ratio 1:4. XRD
296 results reveal that, the green synthesis yields stable, face centered cubic structure AgNPs with a sizes
297 range of 39.664-24.708 nm. Preparation of AgNPs using plant extracts are eco-friendly, biocompatible

298 and cost effective. Generally AgNPs have a vital role in different nanotechnology-based processes
299 because of their unique characteristics and can be exploited on a large scale for medical application. We
300 believe that in the near future a greener and more biosynthesized AgNPs will open many new windows
301 toward biomedical applications. Moreover; further research on AgNPs will provide opportunities in energy
302 storage devices which will solve the current energy crisis globally.

303 **ACKNOWLEDGEMENTS**

304 We are thankful to Axum University, Mekelle University and Addis Pharmaceutical Factory (APF) for
305 providing necessary laboratory facilities and valuable support throughout the work.

306 **AUTHORS' CONTRIBUTIONS**

307 All authors took part in the evaluation of the results, read and approved the final manuscript.

308 **COMPETING INTERESTS**

309 The authors declare that they have no competing interests regarding the publication of this paper!

310 **REFERENCES**

- 311 [1] Mahasneh AM. Bionanotechnology: The Novel Nanoparticles Based Approach for Disease Therapy.
312 Jordan J. Biol. Sci. 2013; 6:246–251.
- 313 [2] Al-Thabaiti SA, Aazam ES, Khan Z, Bashir O. Aggregation of Congo red with surfactants and Ag-
314 nanoparticles in an aqueous solution. Spectrochim. Acta Part A Mol. Biomol. Spectrosc. 2016;
315 156:28–35.
- 316 [3] Paul K, Bag BG, Samanta K. Green coconut (*Cocos nucifera* Linn) shell extract mediated size
317 controlled green synthesis of polyshaped gold nanoparticles and its application in catalysis. Appl.
318 Nanosci. 2014; 4:769–775.
- 319 [4] Khlebtsov NG, Dykman LA. Plasmonic Nanoparticles: Fabrication, Optical Properties, and Biomedical
320 Applications. In Handbook of Photonics for Biomedical Science; CRC Press: Boca Raton, FL, USA.
321 2010; 73–122.
- 322 [5] Muruganandam S, Anbalagan G, Murugadoss G. Optical, electrochemical and thermal properties of
323 Co²⁺-doped CdS nanoparticles using polyvinylpyrrolidone. Appl. Nanosci. 2015; 5:245–253.
- 324 [6] Liu XM, Feng ZB, Zhang FD, Zhang SQ, He XS. Preparation and testing of cementing and coating
325 nanosubnanocomposites of slow/controlled-release fertilizer. Agric. Sci. China 2006; 5:700–706.
- 326 [7] Prathna TC, Sharma SK, Kennedy M. Nanoparticles in household level water treatment: An overview.
327 Sep. Purif. Technol. 2018; 199:260–270.
- 328 [8] Pugazhendhi A, Prabakar D, Jacob JM, Karuppusamy I, Saratale RG. Synthesis and characterization
329 of silver nanoparticles using *Gelidium amansii* and its antimicrobial property against various
330 pathogenic bacteria. Microb. Pathog. 2018; 114:41–45.
- 331 [9] Chatzigoulas A, Karathanou K, Dellis D, Cournia Z. NanoCrystal: A web-based crystallographic tool
332 for the construction of nanoparticles based on their crystal habit. J. Chem. Inf. Model. 2018; 58:2380–
333 2386.

- 334 [10] Atuchin VV, Galashov EN, Khyzhun OY, Kozhukhov AS, Pokrovsky LD, Shlegel VN. Structural and
335 electronic properties of ZnWO₄ (010) cleaved surface. *Cryst. Growth Des.* 2011; 11:2479–2484.
- 336 [11] Korbekandi H, Irvani S. *Silver Nanoparticles*. IntechOpen: London, UK, 2012.
- 337 [12] Kokh KA, Atuchin VV, Gavrilova TA, Kuratieva NV, Pervukhina NV, Surovtsev NV. Microstructural
338 and vibrational properties of PVT grown Sb₂Te₃ crystals. *Solid State Commun.* 2014; 177:16–19.
- 339 [13] Mudavakkat VH, Atuchin VV, Kruchinin VN, Kayani A, Ramana CV. Structure, morphology and
340 optical properties of nanocrystalline yttrium oxide (Y₂O₃) thin films. *Opt. Mater.* 2012; 34:893–900.
- 341 [14] Dorozhkin KV, Dunaevsky GE, Sarkisov SY, Suslyaev VI, Tolbanov OP, Zhuravlev VA, Sarkisov YS,
342 Kuznetsov VL, Moseenkov SI, Semikolenova NV. Terahertz dielectric properties of multiwalled
343 carbon nanotube/polyethylene composites. *Mater. Res. Express.* 2017; 4:106201.
- 344 [15] Sharifi-Rad M, Pohl P, Epifano F. Phytofabrication of Silver Nanoparticles (AgNPs) with
345 Pharmaceutical Capabilities Using *Otostegia Persica* (Burm.) Boiss. Leaf Extract. *Nanomaterials.*
346 2021; 11:1045.
- 347 [16] Singh A, Kaur K. Biological and Physical Applications of Silver Nanoparticles with Emerging Trends of
348 Green Synthesis. *Engineered Nanomaterials - Health and Safety.* 2020; Available:
349 <https://doi.org/10.5772/intechopen.88684>.
- 350 [17] Abass Sofi M, Sunitha S, Ashaq Sofi M, Khadheer Pasha SK, Choi D. An Overview of Antimicrobial
351 and Anticancer Potential of Silver Nanoparticles. *Journal of King Saud University-Science* 2022;
352 34:101791.
- 353 [18] Senapati S, Ahmad A, Khan MI, Sastry M, Kumar R. Extracellular biosynthesis of bimetallic Au–Ag
354 alloy nanoparticles. *Small.* 2005; 1:517–520.
- 355 [19] Klaus-Joerger T, Joerger R, Olsson E, Granqvist CG. Bacteria as workers in the living factory: Metal-
356 accumulating bacteria and their potential for materials science. *Trends Biotechnol.* 2001; 19:15–20.
- 357 [20] Banerjee P, Satapathy M, Mukhopahayay A, Das P. Leaf extract mediated green synthesis of silver
358 nanoparticles from widely available Indian plants: Synthesis, characterization, antimicrobial property
359 and toxicity analysis. *Bioresour. Bioprocess.* 2014; 1:3.
- 360 [21] Sondi I, Salopek-Sondi B. Silver nanoparticles as antimicrobial agent: A case study on *E. coli* as a
361 model for Gram-negative bacteria. *J. Colloid Interface Sci.* 2004; 275:177–182.
- 362 [22] Kuppusamy P, Yusoff MM, Maniam GP, Govindan N. Biosynthesis of metallic nanoparticles using
363 plant derivatives and their new avenues in pharmacological applications—An updated report. *Saudi*
364 *Pharm. J.* 2016; 24:473–484.
- 365 [23] Gurunathan S, Kalishwaralal K, Vaidyanathan R, Venkataraman D, Pandian SRK, Muniyandi J,
366 Hariharan N, Eom SH. Biosynthesis, purification and characterization of silver nanoparticles using
367 *Escherichia coli*. *Colloids Surf. B Biointerfaces* 2009; 74:328–335.
- 368 [24] Narayanan KB, Park HH. Antifungal activity of silver nanoparticles synthesized using turnip leaf
369 extract (*Brassica rapa* L.) against wood rotting pathogens. *Eur. J. Plant Pathol.* 2014; 140:185–192.

- 370 [25] Suriyakalaa U, Antony JJ, Suganya S, Siva D, Sukirtha R, Kamalakkannan S, Pichiah PBT,
371 Achiraman S. Hepatocurative activity of biosynthesized silver nanoparticles fabricated using
372 *Andrographis paniculata*. *Colloids Surf. B Biointerfaces*. 2013; 102:189–194.
- 373 [26] Olaleye MT, Akinmoladun AC, Ogunboye AA, Akindahunsi AA. Antioxidant activity and
374 hepatoprotective property of leaf extracts of *Boerhaavia diffusa* Linn against acetaminophen-induced
375 liver damage in rats. *Food Chem. Toxicol*. 2010; 48:2200–2205.
- 376 [27] AlSalhi MS, Devanesan S, Alfuraydi AA. Green synthesis of silver nanoparticles using *Pimpinella*
377 *anisum* seeds: antimicrobial activity and cytotoxicity on human neonatal skin stromal cells and colon
378 cancer cells. *Int J Nanomed*. 2016; 11:4439–4449.
- 379 [28] Devanesan S, AlSalhi MS, Balaji RV. Antimicrobial and cytotoxicity effects of synthesized silver
380 nanoparticles from *Punica granatum* peel extract. *Nanoscale Res Lett*. 2018; 13:315.
- 381 [29] Bindhu MR, Umadevi M, Esmail GA, Al-Dhabi NA, Arasu MV. Green synthesis and characterization
382 of silver nanoparticles from *Moringa oleifera* flower and assessment of antimicrobial and sensing
383 properties. *J Photochem Photobiol B*. 2020; 205:111836.
- 384 [30] Devanesan S, Ponmurugan K, AlSalhi MS, Al-Dhabi NA. Cytotoxic and antimicrobial efficacy of silver
385 nanoparticles synthesized using a traditional phytoproduct, *Asafoetida* Gum. *Int J Nanomed*. 2020;15:
386 4351–4362.
- 387 [31] Al-Ansari MM, Dhasarathan P, Ranjitsingh AJA, Al-Humaid LA. *Ganoderma lucidum* inspired silver
388 nanoparticles and its biomedical applications with special reference to drug resistant *Escherichia*
389 *coli* isolates from CAUTI. *Saudi J Biol Sci*. 2020; 27:2993–3002.
- 390 [32] Devanesan S, AlSalhi MS, Vishnubalaji R, et al. Rapid biological synthesis of silver nanoparticles
391 using plant seed extracts and their cytotoxicity on colorectal cancer cell lines. *J Clust Sci*. 2014;
392 28:595–605.
- 393 [33] Khan SA, Shahid S, Ayaz A, Alkahtani J, Elshikh MS, Riaz T. Phytomolecules-coated nio
394 nanoparticles synthesis using *abutilon indicum* leaf extract: antioxidant, antibacterial, and anticancer
395 activities. *Int J Nanomed*. 2021; 16:1757–1773.
- 396 [34] Khan SA, Shahid S, Lee CS. Green synthesis of gold and silver nanoparticles using leaf extract of
397 *clerodendrum inerme*; characterization, antimicrobial, and antioxidant activities. *Biomolecules*. 2020;
398 10(6):835.
- 399 [35] Khan SA, Shahid S, Hanif S, Almoallim HS, Alharbi SA, Sellami H. Green synthesis of chromium
400 oxide nanoparticles for antibacterial, antioxidant anticancer, and biocompatibility activities. *Int J Mol*
401 *Sci*. 2021; 22(2):502.
- 402 [36] Veerasamy R, Xin TZ, Gunasagaran S, Xiang TFW, Yang EFC, Jeyakumar N, Dhanaraj SA.
403 Biosynthesis of Silver Nanoparticles Using Mangosteen Leaf Extract and Evaluation of Their
404 Antimicrobial Activities. *J. Saudi Chem. Soc*. 2011; 15:113–120.

- 405 [37] Benakashani F, Allafchian A, Jalali SAH. Green Synthesis, Characterization and Antibacterial Activity
406 of Silver Nanoparticles from Root Extract of *Lepidium Draba* Weed. *Green Chem. Lett. Rev.* 2017;
407 10:324–330.
- 408 [38] Mosaviniya M, Kikhavani T, Tanzifi M, Yaraki MT, Tajbakhsh P, Lajevardi A. Facile Green Synthesis
409 of Silver Nanoparticles Using *Crocus Haussknechtii* Bois Bulb Extract: Catalytic Activity and
410 Antibacterial Properties. *Colloids Interface Sci. Commun.* 2019; 33:100211.
- 411 [39] Prakash P, Gnanaprakasam P, Emmanuel R, Arokiyaraj S, Saravanan M. Green Synthesis of Silver
412 Nanoparticles from Leaf Extract of *Mimusops Elengi*, Linn. For Enhanced Antibacterial Activity
413 Against Multi Drug Resistant Clinical Isolates. *Colloids Surf. B Biointerfaces.* 2013; 108:255–259.
- 414 [40] Nakkala JR, Mata R, Gupta AK, Sadras SR. Green Synthesis and Characterization of Silver
415 Nanoparticles Using *Boerhaavia Diffusa* Plant Extract and Their Anti Bacterial Activity. *Indus. Crop*
416 *Prod.* 2014; 52:562–566.
- 417 [41] Kathiravan V, Ravi S, Ashokkumar S. Synthesis of Silver Nanoparticles from *Melia Dubia* Leaf Extract
418 and Their in Vitro Anticancer Activity. *Spectrochim. Acta A Mol. Biomol. Spectrosc.* 2014; 130:116–
419 121.
- 420 [42] Sadeghi B, Rostami A, Momeni SS. Facile Green Synthesis of Silver Nanoparticles Using Seed
421 Aqueous Extract of *Pistacia Atlantica* and its Antibacterial Activity. *Spectrochim. Acta A Mol. Biomol.*
422 *Spectrosc.* 2015; 134:326–332.
- 423 [43] Swamy MK, Akhtar MS, Mohanty SK, Sinniah UR. Synthesis and Characterization of Silver
424 Nanoparticles Using Fruit Extract of *Momordica Cymbalaria* and Assessment of Their in Vitro
425 Antimicrobial, Antioxidant and Cytotoxicity Activities. *Spectrochim Acta A Mol. Biomol. Spectrosc.*
426 2015; 151:939–944.
- 427 [44] Nouri A, Yaraki MT, Lajevardi A, Rezaei Z, Ghorbanpour M, Tanzifi M. Ultrasonic-assisted Green
428 Synthesis of Silver Nanoparticles Using *Mentha Aquatica* Leaf Extract for Enhanced Antibacterial
429 Properties and Catalytic Activity. *Colloids Interface Sci. Commun.* 2020; 35:100252.
- 430 [45] Ogunbile BO, Labulo AH, Fajemilehin AM. *Ife J. Sci.* 2016 18:245–254.
- 431 [46] Espenti CS, Krishna Rao KSV, Rao KM. Bio-synthesis and Characterization of Silver Nanoparticles
432 Using *Terminalia Chebula* Leaf Extract and Evaluation of its Antimicrobial Potential. *Mater. Lett.* 2016;
433 174:129–133.
- 434 [47] Elemike EE, Fayemi OE, Ekennia AC, Onwudiwe DC, Ebenso EE. Silver Nanoparticles Mediated
435 by *Costus afer* Leaf Extract: Synthesis, Antibacterial, Antioxidant and Electrochemical Properties.
436 *Molecules.* 2017; 22(5):701.
- 437 [48] Gnanavel V, Palanichamy V, Roopan SM. Biosynthesis and Characterization of Copper Oxide
438 Nanoparticles and its Anticancer Activity on Human Colon Cancer Cell Lines (HCT-116). *J.*
439 *Photochem. Photobiol. B.* 2017; 171:133–138.
- 440 [49] Rotimi L, Ojemaye MO, Okoh OO, Okoh AI. *J. Mol. Liq.* 2018; 273:615–625.

- 441 [50] Rautela A, Rani J, Debnath (Das) M. Green Synthesis of Silver Nanoparticles from *Tectona Grandis*
442 Seeds Extract: Characterization and Mechanism of Antimicrobial Action on Different Microorganisms.
443 *J. Anal. Sci. Technol.* 2019; 10:1–10.
- 444 [51] Ndikau M, Noah N, Masika E, Andala D. Green Synthesis and Characterization of Silver
445 Nanoparticles Using *Citrullus lanatus* Fruit Rind Extract. *International Journal of Analytical Chemistry.*
446 2017; 1-9.
- 447 [52] Andrea R, David K. Biological activity of green-synthesized silver nanoparticles depends on the
448 applied natural extracts: a comprehensive study, *International Journal of Nanomedicine.* 2017; 12:
449 871-883.
- 450 [53] Sharm G, Sharm AR, Kurian M. Green synthesis of silver nanoparticle using myristica fragrans
451 (nutmeg) seed extract and its biological activity. *Digest Journal of Nanomaterials and Biostructures.*
452 2014; 9: 325-332.
- 453 [54] Mittal AK, Chisti Y, Banerjee UC. Synthesis of metallic nanoparticles using plant extracts.
454 *Biotechnology Advances.* 2013; 31: 346-356.
- 455 [55] Bar H, Bhui DK, Sahoo GP, Sarkar P, Misra A. Green synthesis of silver nanoparticles:
456 Physicochemical and Engineering Aspects. 2009; 348: 212-216.
- 457 [56] Mittal AK, Bhaumik J, Kumar S, Banerjee UC. Biosynthesis of silver nanoparticles: therapeutic
458 potential. *Journal of Colloid and Interface Science* 2014; 415: 39-47.
- 459 [57] Anamika M, Sanjukta C, Prashant R, Geeta W. Evidence based green synthesis of nanoparticles.
460 *Advanced Materials Letters.* 2012; 3: 519-525.
- 461 [58] Muhammad A, Farooq A, Muhammad R, Saeed A, Umer R. Green Synthesis of Silver Nanoparticles
462 through Reduction with *Solanum xanthocarpum* L. Berry Extract: Characterization, Antimicrobial and
463 Urease Inhibitory Activities against *Helicobacter pylori*. *International Journal of Molecular Sciences.*
464 2012; 13: 9923-9941.
- 465 [59] Daizy P. Green synthesis of gold and silver nanoparticles using *Hibiscus rosa sinensis*. *Physica E:*
466 *Low-dimensional Systems and Nanostructures.* 2010; 42: 1417-1424.
- 467 [60] Sathishkumar M, Sneha K, Won W, Cho W, Kim S, Yun YS. Cinnamon *zeylanicum* bark extract and
468 powder mediated green synthesis of nanocrystalline silver particles and its bactericidal activity.
469 *Colloids and Surfaces.* 2009; 73: 332-338.
- 470 [61] Thamer NA, Almashhedy LA. Green synthesis optimization and characterize of silver nanoparticles
471 using aqueous extract of *Crocus sativus*. L. *IJPBS,* 2014; 5: 759-770.
- 472 [62] Sadowski IH, Maliszewska B, Grochowalska I, Polowczyk T, Kozlecki. Synthesis of silver
473 nanoparticles using microorganisms. *Materials Science.* 2008; 26: 419-424.
- 474 [63] Mittal AK, Bhaumik J, Kumar S, Banerjee UC. Biosynthesis of silver nanoparticles: Elucidation of
475 prospective mechanism and therapeutic potential. *J. Colloid Interface Sci.* 2014; 415: 39-47.
- 476 [64] Dubey SP, Lahtinen M, Sarkka H, Sillanpaa M. Bioprospective of *Sorbus aucuparia* leaf extract in
477 development of silver and gold nanocolloids. *Colloids Surf. B Biointerfaces.* 2010; 80: 26-33.

- 478 [65] Rastogi L, Arunachalam J. Green synthesis route for the size controlled synthesis of biocompatible
479 gold nanoparticles using aqueous extract of garlic (*Allium sativum*). *Advances in Material Letters*.
480 2013; 7:548-555.
- 481 [66] Subramanian R, Subbramaniyan P, Raj V. Antioxidant activity of the stem bark of *Shorea roxburghii*
482 and its silver reducing power. *SpringerPlus*. 2013; 2: 28.
- 483 [67] Dwivedi AD, Gopal K. Biosynthesis of silver and gold nanoparticles using *Chenopodium album* leaf
484 extract. *Colloids Surf. A*. 2010; 369:27-33.
- 485 [68] Christensen L, Vivekanandhan S, Misra M, Mohanty AK. Biosynthesis of silver nanoparticles using
486 *Murraya koenigii* (curry leaf): an investigation on the effect of broth concentration in reduction
487 mechanism and particle size. *Adv. Mat. Lett.* 2011; 2: 429-434.
- 488 [69] Prathna TC, Chandrasekaran N, Raichur AM, Mukherjee A. Biomimetic synthesis of silver
489 nanoparticles by *Citrus limon* (lemon) aqueous extract and theoretical prediction of particle size.
490 *Colloids Surf. B Biointerfaces*. 2011; 82: 152-159.
- 491 [70] Rajoriya P, Misra P, Shukla PK, Ramteke PW. Light regulatory effect on the phytosynthesis of silver
492 nanoparticles using aqueous extract of garlic (*Allium sativum*) and onion (*Allium cepa*) bulb. *Curr. Sci*.
493 2016; 111: 1364-1368.
- 494 [71] Szymczycha-Madeja A, Welna M, Zyrnicki W. Multi-element analysis, Bioavailability and fractionation
495 of herbal tea products. *J Brazil Chem Soc*. 2013; 24:777-787.
- 496 [72] Shamel K, Ahmad MB, Yunus WMZW, Ibrahim NA. Synthesis and Characterization of silver/talc
497 nanocomposites using the wet chemical reduction method. *Int. J. Nanomed*. 2010; 5, 743-751.
- 498 [73] Prasad T, Elumalai E. Bio fabrication of Ag nanoparticles using *Moringa oleifera* leaf extract and their
499 antimicrobial activity. *Asian Pacific Journal Tropical Biomedical*, 2011; 1, 439-442.
- 500 [74] Alaraidh IA, Ibrahim MM, Arabia S, El-Gaaly GA. Evaluation of green synthesis of Ag nanoparticles
501 using *Eruca sativa* and *Spinacia oleracea* leaf extracts and their antimicrobial activity. *Iran. J. Biotech*.
502 2014; 12: 50-55.
- 503 [75] Hoseyni F, Dowlatabadi GA, Maryam MS. Investigation of the antimicrobial effect of silver doped
504 Zinc Oxide nanoparticles. *Nanomed. J*. 2017; 4: 50-54.
- 505 [76] Saba P, Maryam G, Saeid B, Green synthesis of silver nanoparticles using the plant extract of *Salvia*
506 *spinosa* grown in vitro and their antibacterial activity assessment. *Journal of Nanostructure in*
507 *Chemistry*. 2019; 9:1-9.